

A Study on Characteristics and Catalytic Properties of Co/ZrO₂-B Catalysts Towards Methanation

Nithinart Chitpong · Piyasan Prasertthdam ·
Bunjerd Jongsomjit

Received: 15 January 2008 / Accepted: 1 February 2008 / Published online: 15 October 2008
© Springer Science+Business Media, LLC 2008

Abstract The B modification (0.5–3 wt%) on zirconia was found to increase the catalytic activities of Co catalyst during methanation. The B modification resulted in (i) preventing the agglomeration of Co oxide species, and (ii) increasing the dispersion of Co oxide species. Only a slight decrease in C₂–C₄ selectivity was observed.

Keywords Cobalt catalyst · Zirconia · Support · Boron modification · Methanation

1 Introduction

In general, supported catalysts usually consist of three components; (i) a catalytic phase, (ii) a promoter, and (iii) a support or carrier. In fact, the catalytic properties apparently depend on the components as mentioned above. The catalytic phase can be metals, metal oxides, and other metal compounds. These can be employed under the specified catalytic reactions. The catalytic performance can be effectively improved by using a promoter such as a noble metal. Besides the catalytic phase and promoter, it is worth noting that a support could play a crucial role for altering the catalytic performance. Basically, a support material acts as a carrier

for the catalytic phase to be well dispersed on it. However, due to the supporting effect along with dispersion of the catalytic phase, the properties of a catalyst could be altered with various supports used. It is reported that many inorganic supports such as silica (SiO₂) [1], alumina (Al₂O₃) [1–5], titania (TiO₂) [1, 6–11], zirconia (ZrO₂) [5, 6], and zeolites have been extensively studied for years. During recent years zirconia has received much attention from researchers in the fields of heterogeneous catalysis as a support material as well as a catalyst because it is more chemically inert than the classical supports and it may possess different chemical properties such as acidity, basicity, reducing, or oxidizing ability [5, 6, 12–14]. However, it should be noted that the properties of zirconia itself may not be suitable as a sole support for the supported cobalt catalyst. Hence, the modification of the zirconia support would be necessary. It has been reported that some metals, such as boron were used to modify the properties of other supports such as alumina or titania [15–19]. It shows a significant enhancement of catalytic activity of cobalt due to increased cobalt dispersion.

In the present study, the effect of boron modification of zirconia on the characteristics and catalytic properties of zirconia-supported cobalt catalyst during CO hydrogenation was investigated. Experimentally, the boron-modified zirconia was prepared by impregnation of boric acid as the source of boron onto the zirconia support. The amounts of boron loading were varied in the range of 0.5 to 3 wt%. After calcination of the modified support, cobalt nitrate was impregnated onto the modified supports. Then, the catalyst samples were characterized using various techniques. The reaction study on carbon monoxide (CO) hydrogenation was performed in order to evaluate the catalytic activity and selectivity of products.

N. Chitpong · P. Prasertthdam · B. Jongsomjit (✉)
Center of Excellence on Catalysis and Catalytic Reaction
Engineering, Department of Chemical Engineering,
Faculty of Engineering, Chulalongkorn University,
Bangkok 10330, Thailand
e-mail: bunjerd.j@chula.ac.th

2 Experimental

2.1 Materials

2.1.1 B-Modified ZrO₂ Support

The B-modified ZrO₂ supports were prepared by the incipient impregnation method. First, boron was impregnated on the ZrO₂ support [from Aldrich (<5 μm, 99.99%)] using a solution of boric acid (99.99%, Aldrich) to produce B-modified ZrO₂ supports having 0.5, 1, and 3 wt% of B. Then, the B-modified ZrO₂ supports were calcined at 500 °C for 4 h prior to impregnation of cobalt.

2.1.2 Co/B-Modified ZrO₂ Catalyst

Cobalt nitrate [Co(NO₃)₂·6H₂O] was dissolved in deionized water and impregnated on the support as derived above to give a final catalyst with 20 wt% of cobalt. The catalyst precursor was dried at 110 °C for 12 h and calcined in air at 500 °C for 4 h.

2.2 Catalyst Nomenclature

The nomenclature used for the support and catalyst samples in this study is as follows:

ZrB-0: ZrO₂ support without B modification

ZrB-*i*: B-modified ZrO₂ having *i* wt% of B

Co/support: supported cobalt catalyst on various supports as derived above

2.3 Catalyst Characterization

2.3.1 BET Surface Area

BET surface area of the samples after calcination was performed to determine if the total surface area changes upon the various B loadings. It was determined using N₂ adsorption at 77 K in a Micromeritics ASAP 2010.

2.3.2 X-ray Diffraction

XRD was performed to determine the bulk crystalline phases of catalyst following different B loadings. It was conducted using a SIEMENS D-5000 X-ray diffractometer with CuK_α (λ = 1.54439 Å). The spectra were scanned at a rate of 2.4° min⁻¹ in the range 2θ = 20–80°.

2.3.3 Temperature-Programmed Reduction

TPR was used to determine the reduction behaviors of the samples. It was carried out using 50 mg of a sample and a

temperature ramp from 35 to 800 °C at 5 °C/min. The carrier gas was 5% H₂ in Ar. A cold trap was placed before the detector to remove water produced during the reaction. A thermal conductivity detector (TCD) was used to determine the amount of H₂ consumed during TPR [20, 21].

2.3.4 Scanning Electron Microscopy and Energy Dispersive X-ray Spectroscopy

The catalyst granule morphology and elemental distribution were obtained using a Hitachi S-3500N scanning electron microscopy (SEM). The SEM was operated using the back scattering electron (BSE) mode at 20 kV and a working distance (the distance between the sample and the electron beam) of 20 mm. After the SEM micrographs were taken, EDX was performed to determine the elemental concentration distribution on the catalyst granules using INCA software.

2.3.5 Transmission Electron Microscopy

The dispersion of cobalt oxide species on the various supports was determined using a JEOL-TEM 200CX transmission electron microscopy operated at 200 kV with 25 k magnification.

2.3.6 Hydrogen Chemisorption

Static H₂ chemisorption at 100 °C on the reduced samples [at 350 °C for 10 h in H₂ (30 cc/min)] was used to determine the number of reduced surface cobalt metal atoms. This is related to the overall activity of the samples during CO hydrogenation. Gas volumetric chemisorption at 100 °C was performed using the method described by Reuel and Bartholomew [22]. The experiment was performed in a Micromeritics ASAP 2010 using ASAP 2010C V3.00 software.

2.4 Reaction Study

Methanation (H₂/CO = 10/1) was performed to determine the overall activity of the catalyst samples reduced at various conditions. Methanation was carried out at 220 °C and 1 atm. A flowrate of H₂/CO/Ar = 20/2/8 cc min⁻¹ in a fixed-bed flow reactor was used. A relatively high H₂/CO ratio was used to minimize deactivation due to carbon deposition during reaction. Typically, 20 mg of a catalyst sample was reduced in situ in flowing H₂ (30 cc min⁻¹) at 350 °C for 10 h prior to the reaction. Reactor effluent samples were taken at 1 h intervals and analyzed by GC. In all cases, steady-state was reached within 5 h.

3 Results and Discussion

The present study focused on the effect of boron (B) modification on zirconia-supported cobalt catalysts for methanation. The BET surface area and cobalt oxide crystallite size obtained from the XRD measurement using Scherrer's equation [22] are listed in Table 1. The BET surface areas of B-modified zirconia supports decreased from 2.6 to 1.1 m²/g upon increasing the amounts of boron loading. The pore size distributions of the unmodified and B-modified zirconia support are shown in Fig. 1. In fact, the slightly bimodal pore size distribution for the unmodified zirconia support was observed. However, with the B modification, the unimodal pore size distribution of the B-modified zirconia supports was evident. It indicated that B was presumably located in the small pore of zirconia support resulting in the disappearance of the small pore portion as

Table 1 Characteristics of supports and catalysts

Samples	BET Surface Area (m ² /g) ^a	XRD Co oxide crystallite size ^b (nm)	TEM Co oxide particle size ^c (nm)
ZrB-0	2.6	—	—
ZrB-0.5	1.8	—	—
ZrB-1	1.3	—	—
ZrB-3	1.1	—	—
20-Co/ZrB-0	1.8	59.6	259
20-Co/ZrB-0.5	6.8	55.0	236
20-Co/ZrB-1	12.4	32.1	207
20-Co/ZrB-3	12.6	11.6	159

^a Measurement error is ±5%

^b Determined by XRD line broadening using Scherrer's equation [23]

^c Derived from the measurement of average particle size as seen by TEM micrographs

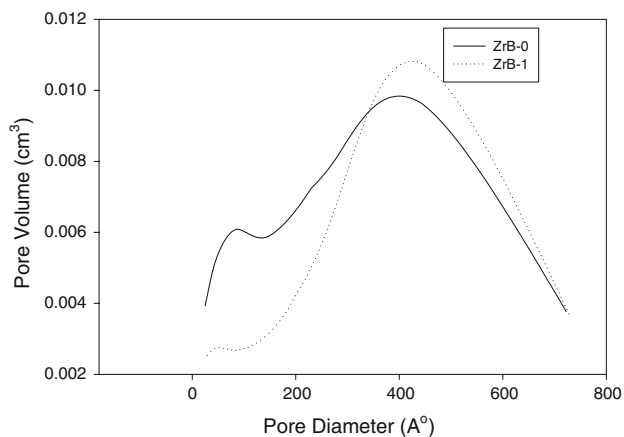


Fig. 1 Pore size distribution of supports

seen in Fig. 1. Considering the surface areas of the zirconia-supported cobalt catalysts with B modification, they apparently increased from 1.8 to 12.6 m²/g with increasing the amounts of B loading in the zirconia supports. This was suggested that the B modification could prevent the agglomeration of Co oxide species resulting in increased surface areas of the catalyst samples. The XRD patterns for different zirconia supports consisting of various amounts of boron loading are shown in Fig. 2. The unmodified zirconia support exhibited the strong XRD peaks at 29° and 32° assigning to the ZrO₂ in the monoclinic phase, and the strong XRD peak at 50° indicating the ZrO₂ in the tetragonal phase. In addition, the strong XRD peak at 29° (overlap with the XRD peak for the monoclinic phase of ZrO₂) was detected for the zirconia supports with B modification also assigning to the B₂O₃ species [24]. Figure 3 shows the XRD patterns of different zirconia-supported cobalt catalysts consisting of

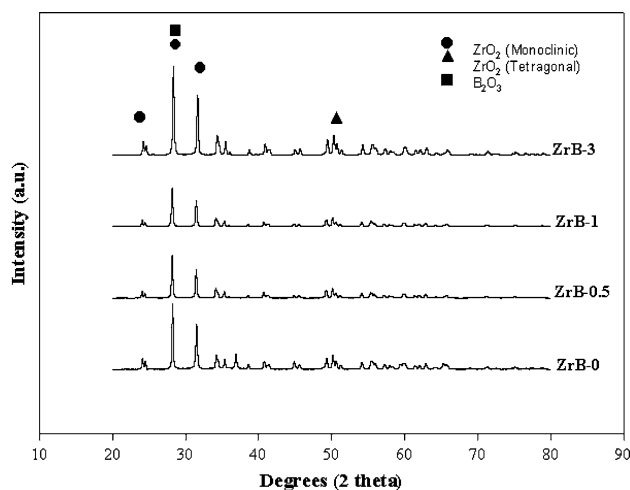


Fig. 2 XRD patterns for different ZrO₂ supports consisting of various amounts of boron loading

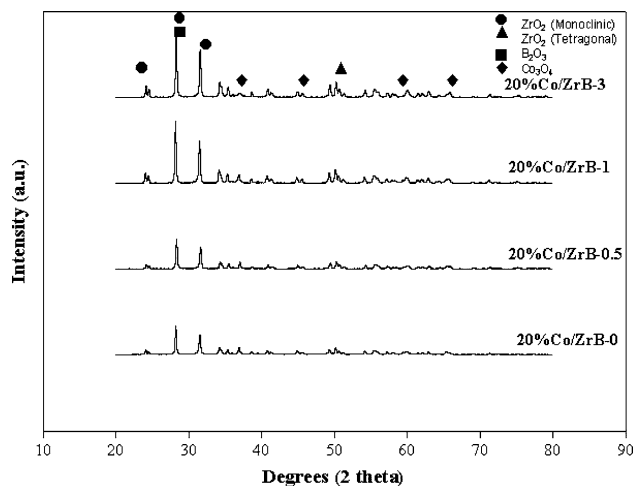


Fig. 3 XRD patterns for different Co/ZrO₂ catalysts with various amounts of boron modification on zirconia support

various amounts of B loading in the zirconia supports. The catalyst samples exhibited XRD peaks at 36° , 45° , 60° and 65° indicating the presence of Co_3O_4 species. The XRD crystallite size of cobalt catalysts decreased from 59.6 to 11.6 nm upon increasing the amounts of B loading indicating high Co oxide dispersion with the B modification on zirconia support. This result was in accordance with the obtained surface areas as mentioned above.

In order to study the morphologies and elemental distribution of the catalyst samples, SEM and EDX were performed, respectively. The SEM micrograph and the elemental distribution for Co, Zr, and O for the unmodified zirconia-supported Co catalyst are shown in Fig. 4 whereas the typical SEM micrograph and the elemental distribution for the B-modified zirconia-supported Co catalyst are shown in Fig. 5. For both figures, it was found that the distribution of Co oxide species was well distributed all over the catalyst granule. In order to determine the dispersion and crystallite size of Co oxides species dispersed on the various supports employed, the high resolution TEM was used. The TEM micrographs for the unmodified and B-modified zirconia supports are shown in Fig. 6. There was no significant change in morphologies of the zirconia supports upon B modification. The dispersion of Co oxide species on various zirconia supports is illustrated in Fig. 7. It can be observed that the dispersion of Co oxide species apparently increased with increasing the amounts of B

loading in the zirconia support resulting in the smaller size of the Co oxides present. The TEM results were in agreement with we have found using the XRD measurement as mentioned before. As seen from Table 1, the crystallite size obtained from XRD measurement of the Co oxide species decreased from 59.6 to 11.6 nm upon increasing the amount of B loading from 0.5 to 3 wt% into the zirconia support. Considering the Co oxide sizes obtained from the TEM measurement as also listed in Table 1, they apparently ranged between 159 and 259 nm. The Co oxide sizes also decreased with the B modification as observed by XRD. However, when compared the Co oxide sizes obtained from XRD and TEM measurement, it was found that the sizes obtained from the TEM were much larger (about an order of magnitude). This was due to the agglomeration of the primary particles into the secondary particles as seen by the TEM used in this study.

The TPR measurement was performed in order to determine the reduction behaviors of Co oxides species on various samples. The TPR profiles of various zirconia-supported Co catalysts with and without B modification on zirconia supports are shown in Fig. 8 and the reduction temperatures are listed in Table 2. Basically, only two reduction peaks can be observed. The peaks can be assigned to the two-step reduction of Co_3O_4 to CoO and then to Co^0 [21, 25]. Upon the TPR conditions, the two reduction peaks based on two-step reduction may or may

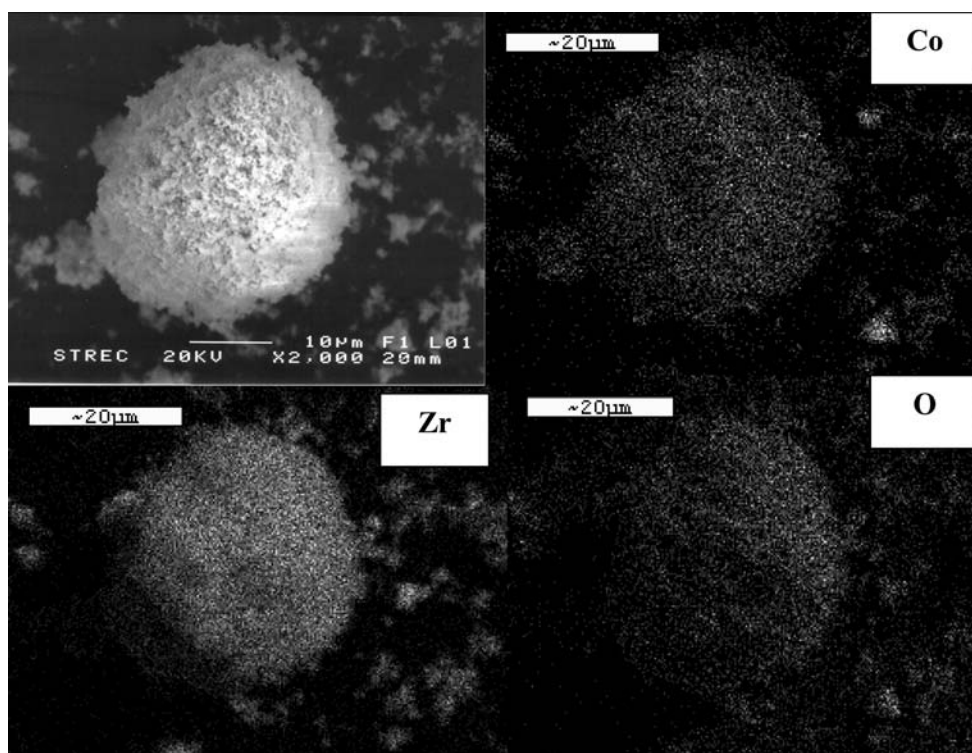


Fig. 4 A typical SEM micrograph and EDX mapping for 20-Co/ZrB-0 sample

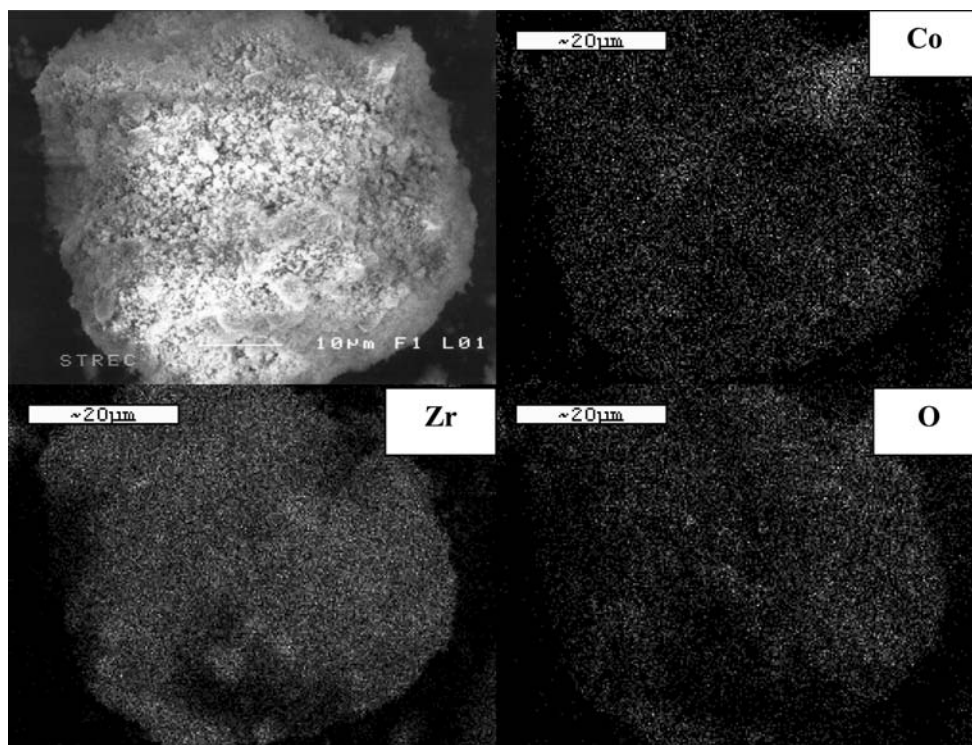


Fig. 5 A typical SEM micrograph and EDX mapping for 20-Co/ZrB-3 sample

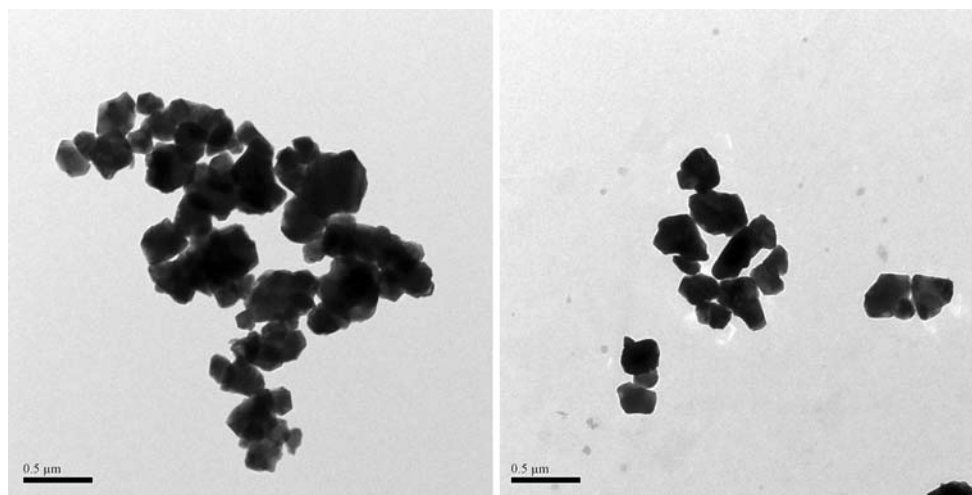


Fig. 6 TEM micrographs for different ZrO₂ supports consisting of various amounts of boron loading; ZrB-0 (Left) and ZrB-3 (Right)

not be observed. Here, for the unmodified zirconia-supported Co catalyst, the broad reduction peak (ca. 230–490 °C) having a little shoulder (ca. 300 °C) can be observed assigning to the overlap of two-step reduction. However, with the B modification we found that the reduction peaks were shifted to the higher reduction temperatures. The reducibility during TPR (30–800 °C) as also shown in Table 2 were in the range of 18.9 to 22.3%. It was suggested that the B-modification can result in lower

degree of reduction, especially with high amounts (3 wt%) of B loading on the zirconia supports. The smaller size of Co oxide species, the more difficult of them to be reduced. However, it should be noted that TPR conditions were different from the standard reduction used prior to reaction. Therefore, the H₂ chemisorption was performed in order to determine the number of reduced cobalt metal surface atoms. It is known that the active form of cobalt catalysts for CO hydrogenation is cobalt metal (Co⁰). Thus,

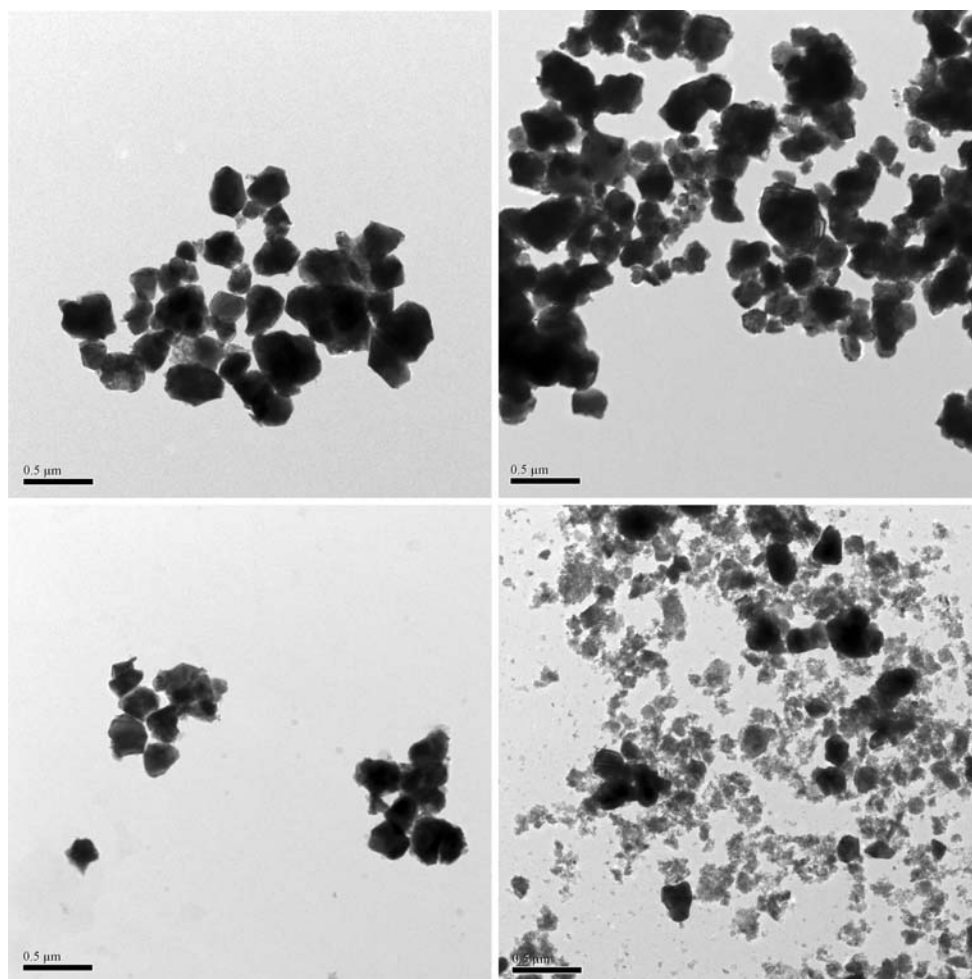


Fig. 7 TEM micrographs for different Co/ZrO₂ catalysts with various amounts of boron modification on zirconia support; 20Co/ZrB-0 (Top-Left), 20Co/ZrB-0.5 (Top-Right), 20Co/ZrB-1 (Bottom-Left) and 20Co/ZrB-3 (Bottom-Right)

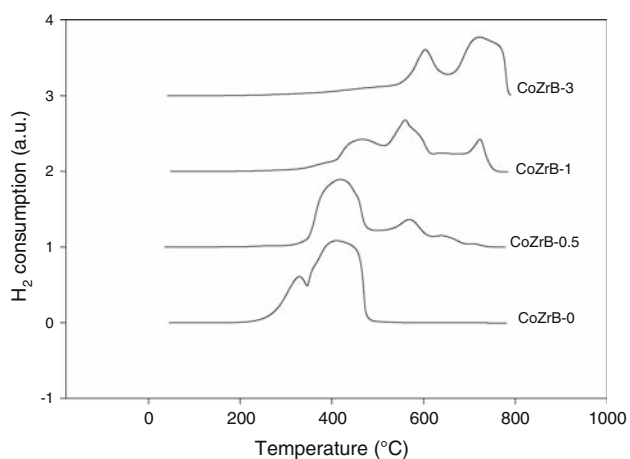


Fig. 8 TPR profiles for different Co/ZrO₂ catalysts with various amounts of boron modification on zirconia support

reduction of cobalt oxide species is essentially performed in order to transform cobalt oxides obtained after calcination process into the active cobalt metal atoms for

Table 2 Reduction temperature of catalyst samples

Catalyst samples	Reduction temperature (°C)			% Reducibility during TPR (30–800 °C) ^a
	Initial	Final	Maximum	
20-Co/ZrB-0	230	490	420	22.3
20-Co/ZrB-0.5	330	760	450	19.8
20-Co/ZrB-1	350	770	570	18.9
20-Co/ZrB-3	560	800	750	19.8

^a Based on the peak areas below TPR curve

Table 3 H₂ chemisorption and % cobalt dispersion

Catalyst samples	Total H ₂ chemisorption (μmol H ₂ /g cat)	Cobalt dispersion (%)
20-Co/ZrB-0	0.33	1.9
20-Co/ZrB-0.5	0.44	2.6
20-Co/ZrB-1	0.47	2.8
20-Co/ZrB-3	0.34	2.0

Table 4 Activities and selectivity of various catalysts during CO hydrogenation

Catalyst samples	CO conversion (%)	Steady-state rate ^a (x10 ² gCH ₂ /g cat h)	CH ₄ selectivity (%)	C ₂ –C ₄ selectivity (%)	TOF _H ^b (s ⁻¹)
20-Co/ZrB-0	8	3.0	96.5	3.5	0.36
20-Co/ZrB-0.5	54	20.2	99.0	1.0	1.82
20-Co/ZrB-1	68	25.2	99.0	1.0	2.13
20-Co/ZrB-3	61	22.7	98.9	1.1	2.66

^a Methanation was carried out at 220 °C, 1 atm and H₂/CO/Ar = 20/2/8. The steady-state was reached after 5 h

^b Based on the H₂ chemisorption

catalyzing the reaction. Hence, the static H₂ chemisorption on the reduced cobalt samples (at the same condition used to reduce the catalyst samples prior to reaction) was used to determine the number of cobalt metal surface atoms. This is usually related to the overall activity of the catalyst during CO hydrogenation. The H₂ chemisorption results are shown in Table 3 indicating increased Co dispersion upon the B modification.

The reaction study under methanation was also investigated in order to measure the activity and selectivity of catalysts. The reaction study results are listed in Table 4. The CO conversion ranged between 8 and 68% upon the B modification. It was obvious that the catalytic activities of the zirconia-supported Co catalyst dramatically increased about 6–8 times with B-modification on the zirconia supports. Increased activities upon B-modification can be attributed to increased dispersion of Co oxide species as seen from the XRD and TEM measurements. This was suggested that the higher degree dispersion of Co oxide species could facilitate the reduction of Co oxides giving the higher number of the Co metal surface atoms for catalyzing the reaction. However, it should be carefully noted that too small crystallite sizes of Co oxides, i.e., 11.6–32.1 nm (obtained from the XRD measurement), which were corresponding to the amounts of B loading of 0.5 and 3 wt%, respectively essentially decreased the degree of reduction resulting in a slight decrease in activity. It was interesting to note that the rate increased from 20-Co/ZrB-0 to 20-Co/ZrB-0.5, but the rate was more constant for 20-Co/ZrB-0.5, 20-Co/ZrB-1, and 20-Co/ZrB-3. However, the Co oxide sizes (based on XRD) decreased from 55 nm for 20-Co/ZrB-0.5 to 32 nm for 20-Co/ZrB-1, and to 11.6 nm for 20-Co/ZrB-3. It should be mentioned that XRD was used to measure the size of Co oxide species, not the reduced Co metal atoms. This suggested that the sizes of Co oxide species was the only factor that insured larger number of reduced Co metal atoms [10]. In fact, the kinetics of reduction can be affected by a wide range of variables, including crystallite size, support interaction, and reduction gas composition

[2–4]. The effects of crystallite size and support interaction can be superimposed on each other. Thus, while a decrease in metal oxide crystallite size can result in faster reduction due to greater surface area/volume ratio, smaller particles may interact more with the support, slowing reduction. The similar phenomenon was also discussed for the dispersion of Co oxide species on titania supports consisting of various ratios of anatase and rutile phases [9, 10, 26]. Thus, this was also confirmed that highly dispersed forms of Co oxide species were not only the factor to insure larger number of reduced Co metal surface atoms. Considering the product selectivity upon methanation condition as seen in Table 4, it was found that the selectivity to C₂–C₄ products slightly decreased with the B modification on the zirconia supports. The TOF values (0.36–2.66 s⁻¹) calculated on the basis of H₂ chemisorption for all samples are also shown in Table 4. It indicated that the enhanced activities during methanation for the catalyst samples with B modification were apparently attributed to increased TOF values (about an order of magnitude). Yamasaki et al. [27] reported on the use of Ni/ZrO₂ catalysts under similar methanation condition. They found that the TOF values ranged between 0.73 and 5.43 s⁻¹. These were similar to the TOF values reported in this work, which were typical for the cobalt catalyst under this condition.

4 Conclusions

It appeared that B modification on the zirconia supports resulted in increased activities based on methanation without a dramatic change in the product selectivity. The increased activities can be attributed to higher dispersion of Co oxide species on the support. It was suggested that the role of B modification could be drawn based on (i) preventing the agglomeration of Co oxide species and (ii) increasing the dispersion of the Co oxide species, then facilitating reduction of Co oxides to Co metal surface atoms for catalyzing the reaction.

Acknowledgments We thank the Thailand Research Fund (TRF) for RMU50-B. Jongsomjit and the graduate school at Chulalongkorn University (90th Anniversary of CU under the Golden Jubilee Fund) for financial support of this project.

References

1. Jacobs G, Das T, Zhang Y, Li J, Racoillet G, Davis BH (2002) *Appl Catal A: Gen* 233:263
2. Jongsomjit B, Panpranot J, Goodwin JG Jr (2001) *J Catal* 204:98
3. Jongsomjit B, Goodwin JG Jr (2002) *Catal Today* 77:191
4. Jongsomjit B, Panpranot J, Goodwin JG Jr (2003) *J Catal* 215:66
5. Enache DI, Auberger MR, Revel R (2004) *Appl Catal A: Gen* 268:51
6. Kraum M, Baerns M (1999) *Appl Catal A: Gen* 186:189
7. Madikizela NN, Coville NJ (2002) *J Mol Catal A: Chem* 181:129
8. Jongsomjit B, Sakdamnusun C, Goodwin JG Jr, Prasertthdam P (2004) *Catal Lett* 94:209
9. Jongsomjit B, Sakdamnusun C, Prasertthdam P (2005) *Mater Chem Phys* 89:395
10. Jongsomjit B, Wongsalee T, Prasertthdam P (2005) *Mater Chem Phys* 92:572
11. Wongsalee T, Jongsomjit B, Prasertthdam P (2006) *Catal Lett* 108:55
12. Panpranot J, Taochaiyaphum N, Prasertthdam P (2005) *Mater Chem Phys* 89:395
13. Panpranot J, Taochaiyaphum N, Jongsomjit B, Prasertthdam P (2006) *Catal Commun* 7:192
14. Soisuwan P, Prasertthdam P, Panpranot J, Trimm DL (2006) *Catal Commun* 7:761
15. Stranick MA, Houalla M, Hercules DM (1987) *J Catal* 104:396
16. Li J, Coville NJ (1999) *Appl Catal A: Gen* 181:201
17. Li J, Coville NJ (2002) *Catal Today* 71:403
18. Li J, Jacobs G, Zhang Y, Das T, Davis BH (2002) *Appl Catal A: Gen* 223:195
19. Brik Y, Kacimi M, Verduraz FB, Ziyad MJ (2002) *J Catal* 211:470
20. Kogelbaue A, Weber JC, Goodwin JG Jr (1995) *Catal Lett* 34:269
21. Zhang Y, Wei D, Hammache S, Goodwin JG Jr (1999) *J Catal* 188:281
22. Reuel RC, Bartholomew CH (1984) *J Catal* 85:63
23. Klug HP, Alexander LE (1974) *X-ray diffraction procedures for polycrystalline amorphous*, 2nd edn. Wiley, New York
24. Tupabut P, Jongsomjit B, Prasertthdam P (2007) *Catal Lett* 118:195
25. Schanke D, Vada S, Blekkan EA, Hilmen A, Hoff A, Holmen A (1995) *J Catal* 156:85
26. Jongsomjit B, Wongsalee T, Prasertthdam P (2005) *Catal Commun* 6:705
27. Yamasaki M, Habasaki H, Asami K, Izumiya K, Hashimoto K (2006) *Catal Commun* 7:24